Inorganic Chemistry

Article

pubs.acs.org/IC

Structures and Stability of Molecular $InBr_3Py_x$ (x = 1−3) Complexes: Unexpected Solid State Stabilization of Dimeric $In_2Br_6Py_4$ As Compared to Valence-Isoelectronic Group 15 and 17 Halogen Bridging Dimers

Igor V. Kazakov,[†] Michael Bodensteiner,[‡] Anna S. Lisovenko,[†] Andrew V. Suvorov,[†] Manfred Scheer,[‡] Gábor Balázs,[‡] and Alexey Y. Timoshkin*[,†]

[†]Inorganic Chemistry Group, Department of Chemistry, St. Petersburg State University, University Pr. 26, Old Peterhof, St. Petersburg 198504, Russia

[‡]Department of Inorganic Chemistry, University of Regensburg, 93040 Regensburg, Germany

Supporting Information

ABSTRACT: Molecular structures of series of $InBr_3Py_x$ complexes (x = 1−3) in the solid state have been determined by single crystal structure analysis. For x = 2, an unexpected dimeric $In_2Br_6Py_4$ structure, which features a nearly planar In_2Br_6 unit, has been established. This structure completes the series of known valence-isoelectronic dimeric molecules of group 17 (I_2Cl_6) and group 15 elements (As_2Cl_6·$2PMe_3$). Theoretical studies at the B3LYP/def2-TZVP level of theory reveal that all gaseous $M_2X_6Py_4$ dimers (M = Al, Ga, In, Tl; X = Cl, Br) are energetically unstable with respect to dissociation into MX_3Py_2 monomers. This finding is in stark contrast to the valence-isoelectronic group 17 and 15 analogs, which are predicted to be energetically stable with respect to dissociation. Thus, additional interactions in the solid state play a crucial role in stabilization of the experimentally observed dimeric $In_2Br_6Py_4$. Thermal stability and volatility of $InBr_3Py_x$ complexes have been studied by tensimetry and mass spectrometry methods. Mass spectrometry data indicate that, in contrast to the lighter group 13 element halides, species with two In atoms, such as $In_2Br_6Py_2$, are present in the gas phase. Thermodynamic characteristics for the heterogeneous dissociation processes of $InBr_3Py_x$ (x = 2, 3) complexes with Py evolution have been determined.

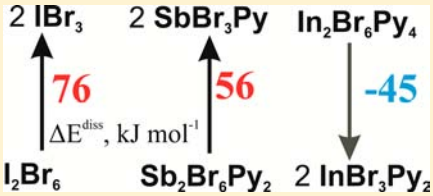

INTRODUCTION

Group 13 metal halides are typical Lewis acids that have numerous applications in modern chemistry. Complexes with group 15 Lewis bases[1,2] are prospective precursors for chemical vapor deposition (CVD) of group 13−15 materials.[3] Volatility and stability are key features for a successful precursor. The structure of the precursor in the solid state plays a decisive role on its volatility. Complexes with molecular structures are expected to have higher volatility than ionic or polymeric compounds. One of the crucial factors affecting the complex stability is the energy of the donor−acceptor (DA) bond. Pyridine is a useful model ligand for experimental studies of DA bond breaking because it is thermally stable and easily forms adducts with group 13 element halides MX_3Py_x (x = 1−3). Complexes with x = 1 are the most abundant; they possess molecular MX_3Py structures.[1,2,4−6] Complexes with two pyridine molecules exist as either trigonal bipyramidal molecules MX_3Py_2 or ionic compounds $[MX_2Py_4]^+[MX_4]^-$, whereas complexes with x = 3 form molecular octahedrons MX_3Py_3.[7−9,11−14] Despite many structural studies, only one series of $AlCl_3Py_x$ (x = 1−3) complexes was fully structurally characterized.[6,8]

In contrast to lighter group 13 metals, which usually adopt coordination number 4, indium prefers coordination number 6.[15] Such a tendency leads to the formation of a variety of complexes with unusual structural motifs, for example, in the recently characterized molecular complex $[(InCl_3)_4\{o\text{-}C_6H_4(CH_2SEt)_2\}_3]$.[16] Synthesis of $InBr_3Py_2$ and $InBr_3Py_3$ in acetonitrile solution has been reported, but no structural information is available.[17] Structurally characterized indium(III) halide complexes with pyridine are limited to series of tris adducts: $InCl_3Py_3$·Py,[11] $InBr_3Py_3$·Py,[12] and InI_3Py_3.[13] Apparently, there are no structural data on mono and bis adducts of indium halides with pyridine.

Herein, we report the solid state structures, thermal stability, and volatility of a complete series of indium bromide−pyridine complexes, $InBr_3Py_x$ (x = 1−3). We demonstrate that the complex with x = 2 exists in the solid state in the unusual dimeric form $In_2Br_6Py_4$. This unexpected structure prompted us to perform theoretical studies of $M_2X_6Py_4$ dimers (M = Al, Ga, In, Tl; X = Cl, Br) and their valence-isoelectronic analogs of group 17 and 15 element halides. The results of these studies are also presented and discussed.

Received: August 23, 2013
Published: November 7, 2013

   dx.doi.org/10.1021/ic402162d | Inorg. Chem. 2013, 52, 13207−13215

Table 1. Crystal Structure Information for Investigated Complexes

complex	$InBr_3Py$ (**1**)	$InBr_3Py_2$ (**2**)	$InBr_3Py_3$ (**3**)	I_2Cl_6 (**4**)
empirical formula	$C_5H_5Br_3InN$	$C_{20}H_{20}Br_6In_2N_4$	$C_{15}H_{15}Br_3InN_3$	Cl_6I_2
M_r	433.62	1025.44	591.82	466.50
crystal system	orthorhombic	orthorhombic	orthorhombic	triclinic
space group	*Pbca*	*Fddd*	*Pbcn*	$P\bar{1}$
a (Å)	13.2768(4)	14.6209(4)	9.3125(1)	5.4020(3)
b (Å)	11.2949(4)	15.5436(5)	15.0076(2)	5.6323(3)
c (Å)	13.6333(6)	25.6230(8)	13.4349(2)	8.3070(4)
α (deg)	90	90	90	71.756(5)
β (deg)	90	90	90	78.314(5)
γ (deg)	90	90	90	81.092(5)
V (Å^3)	2044.45(13)	5823.1(3)	1877.64(4)	233.93(2)
Z	8	8	4	1
T (K)	123(1)	123(1)	123(1)	123(1)
crystal color/shape	colorless block	colorless block	colorless plate	yellow plate
crystal size (mm^{-3})	0.40 × 0.21 × 0.11	0.16 × 0.14 × 0.09	0.18 × 0.11 × 0.11	0.27 × 0.10 × 0.03
ρ_{calcd} (g/cm^3)	2.818	2.339	2.094	3.311
$F(000)$	1568	3808	1120	208
μ (mm^{-1})	31.706	22.435	17.528	8.348
T_{min}/T_{max}	0.191/1.000	0.114/0.295	0.678/1.000	0.298/0.806
abs corr type	multiscan	analytical	multiscan	Gaussian
wavelength λ (Å)	1.54178 (Cu Kα)	1.54178 (Cu Kα)	1.54178 (Cu Kα)	0.71073 (Mo Kα)
reflns coll/uniq (R_{int})	6946/1763 (0.0574)	4880/1185 (0.0590)	17314/1653 (0.0300)	9677/1975 (0.0375)
uniq reflns $I > 2\sigma(I)$	1687	975	1621	1727
index range	$-15 \le h \le 14$	$-16 \le h \le 16$	$-11 \le h \le 10$	$-8 \le h \le 8$
	$-13 \le k \le 13$	$-17 \le k \le 17$	$-17 \le k \le 17$	$-9 \le k \le 9$
	$-14 \le l \le 15$	$-25 \le l \le 29$	$-15 \le l \le 15$	$-13 \le l \le 13$
$\theta_{min} - \theta_{max}$ (deg)	6.08−66.56	4.50−63.25	5.59−66.91	3.828−34.964
completeness to θ_{max}	0.977	0.992	0.989	0.989
data/restraints/param	1763/0/91	1185/0/74	1653/0/102	1975/0/37
R values (all data)	R_1 = 0.0737, wR_2 = 0.1910	R_1 = 0.0405, wR_2 = 0.1027	R_1 = 0.0171, wR_2 = 0.0439	R_1 = 0.0206, wR_2 = 0.0365
R values ($I > 2\sigma(I)$)	R_1 = 0.0726, wR_2 = 0.1884	R_1 = 0.0363, wR_2 = 0.0984	R_1 = 0.0166, wR_2 = 0.0435	R_1 = 0.0267, wR_2 = 0.0372
GOF on F^2	1.082	1.179	0.950	0.999
largest diff $\Delta\rho$ (e Å^{-3})	+3.514/−1.375	+1.456/−1.759	+0.338/−0.523	+1.32/−0.67

EXPERIMENTAL DETAILS

Synthetic Procedures. Due to the high sensitivity of $InBr_3$ and its complexes to moisture, all operations have been performed in a sealed whole glass apparatus under vacuum. $InBr_3$ has been synthesized by the direct reaction between the elements and purified by multiple (no less than four times) resublimations in vacuum at 570−580 K. Pyridine was degassed under vacuum by repetition of freezing/melting cycles, stored above zeolites in a sealed glass ampule for no less than 2 weeks, and distilled under vacuum before use. Purity was controlled by mass spectrometry and tensimetry measurements.

*Complex $InBr_3Py$ (**1**).* Pyridine (9.5 mg, 0.12 mmol) was condensed in vacuum to $InBr_3$ (44.5 mg, 0.125 mmol) by cooling in a liquid nitrogen bath. Reaction volume was sealed and kept at 440−450 K for 24 h.

*Complex $InBr_3Py_2$ (**2**).* Pyridine (57.4 mg, 0.726 mmol) was condensed in vacuum to $InBr_3$ (137.5 mg, 0.388 mmol) by cooling in a liquid nitrogen bath. Reaction volume was sealed and kept at 370−380 K for 24 h.

*Complex $InBr_3Py_3$ (**3**).* Pyridine (81.1 mg, 1.03 mmol) was condensed in vacuum to $InBr_3$ (125.2 mg, 0.353 mmol) by cooling in a liquid nitrogen bath. Reaction volume was sealed and stored at 370−380 K for 24 h. Single crystals of **2** and **3** were obtained in different parts of the reaction ampule after 6 weeks at 330−340 K. I_2Cl_6 (**4**) was synthesized from elements under argon atmosphere. I_2 (253.0 mg, 0.996 mmol) in a Schlenk tube under argon was treated with an excess of gaseous chlorine. Single crystals, suitable for X-ray analysis, were obtained by sublimation at room temperature over several days.

X-ray Crystal Structure Analyses of the Complexes. Analyses of the complexes were performed on an Agilent Technologies (formerly Oxford Diffraction) Gemini R Ultra CCD. Either semi-empirical[18] or analytical absorption corrections from crystal faces[19] were applied. The structures were solved by direct methods with the program SIR-97.[20] Full matrix least-squares refinements on F^2 in SHELXL-97 were carried out.[21] The crystal of **1** was twinned. The data were detwinned with an overlap constraint of 0.8 employing the CrysAlis software,[18] and only the major component was used for refinement. The remaining increased residual density is located close to the indium atoms. CCDC 957189, 957190, 957191, and 957192 contain the supplementary crystallographic data for this paper. These data can be obtained free of charge from the Cambridge Crystallographic Data Center via http://www.ccdc.cam.ac.uk/products/csd/request/. Powder diffraction measurements were performed on the powder diffractometer Bruker D2 Phaser at SPbSU Research Centre for X-ray Diffraction Studies.

Quantum Chemical Computations. All computations were performed using density functional theory (DFT) hybrid functional B3LYP[23,24] in conjunction with a triple-ζ quality Ahlrichs def2-TZVP basis set[25] (all electrons for H, C, N, Al, Cl, Ga, As, Br; effective core potentials for In, Sb, I, Tl). The B3LYP method has been successfully applied for the complexes of group 13 metal halides with ammonia[26] and other donors[5] and provided good agreement with high temperature thermodynamic data and satisfactory structural data. Structures of all compounds were fully optimized and verified to be minima or (in several cases) higher order stationary points on their respective potential energy surfaces (PES). The GAUSSIAN 09 program package[27] was used throughout.

RESULTS AND DISCUSSION

Structural Features of $InBr_3Py_x$ (x = 1−3). Experimental details on crystal structure for all complexes are presented in Table 1. In the solid state, **1** adopts the molecular structure $InBr_3Py$ with tetrahedral environment on the In atom revealing coordination number 4 (Figure 1). This compound is

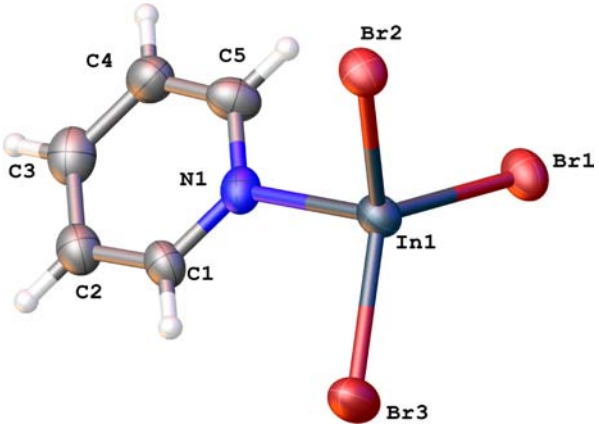

Figure 1. Molecular structure of complex $InBr_3Py$ (**1**) in the crystal. Selected interatomic distances (Å): In1−N1 2.194(7), In1−Br1 2.4855(11), In1−Br2 2.4697(10), In1−Br3 2.4690(11). Selected bond angles (deg): Br1−In1−Br2 110.08(4), Br1−In1−Br3 119.03(4), Br2−In1−Br3 118.74(4), N1−In1−Br1 99.04(18), N1−In1−Br2 103.47(18), N1−In1−Br3 102.61(18).

isostructural to its aluminum and gallium analogs $MX_3{\cdot}Py$ (M = Al, Ga; X = Cl, Br).[5,6] Compared to complexes of lighter group 13 analogs, the donor−acceptor bond distance in **1** (2.194(7) Å) increases by about 0.16 Å in line with the increase of the covalent radii. Similar In−N distances are reported for other $InBr_3$ adducts with other N-containing donors: 2.158(8) Å in $InBr_3{\cdot}N(SnMe_3)_3$[28] and 2.210(9) Å in $InBr_3{\cdot}NH_2SiMe_3$.[29]

Unexpectedly, **2** turned out to be a dimer $In_2Br_6Py_4$ (Figure 2), featuring a planar In_2Br_6 unit with two bridging Br atoms, all four Py molecules occupy axial positions, and the coordination number of In equals 6. This structural type is markedly different from other complexes of group 13 trihalides of 1:2 composition, which adopt either monomeric molecular structures with coordination number 5 (for example, $TlBr_3{\cdot}2Py$[7]), or ionic structures like $[AlCl_2Py_4]^+[AlCl_4]^-$ and $[GaCl_2Py_4]^+[GaCl_4]^-$.[8,9] This is only the second example of such structural type among group 13 element halides: the first was observed for $Tl_2Cl_6L_4{\cdot}2L$ (L = *N*-nicotinamide).[10] The pyridine units in **2** are distorted toward the center of the molecule, the N−In−N angles being 171°. Note that all four pyridine molecules are aligned in a perpendicular fashion with respect to the In−In axis. Such an arrangement allows intramolecular $\pi-\pi$ interaction between the pyridine rings.

The planar In_2Br_6 motif found in **2** can be also seen in the solid state structure of low volatile indium tribromide itself.[30] In contrast to Al_2Br_6 and Ga_2Br_6, which exist in the condensed phase as individual dimeric molecules,[31] solid indium tribromide is a coordination polymer, the coordination number (c.n.) of In equals 6. The structure can be seen as planar In_2Br_6 dimers, each indium additionally coordinated by two bromine atoms from other dimers completing the octahedral coordination sphere. Experimental In−Br distances are in the range 2.643−2.674 Å.

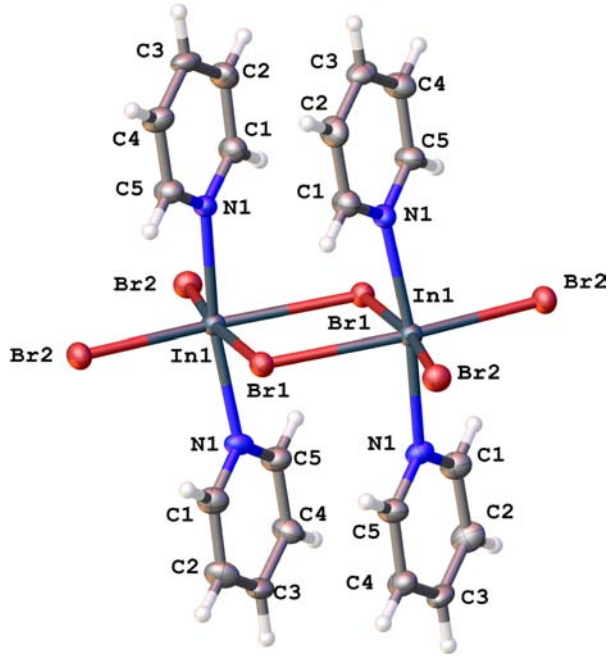

Figure 2. Molecular structure of complex $InBr_3Py_2$ (**2**) in the crystal. Selected interatomic distances (Å): In1−N1 2.275(5), In1−Br1 2.7609(6), In1−Br2 2.5857(6). Selected bond angles (deg): In1−Br1−In1 96.739(3), Br1−In1−Br2 88.84(2), Br2−In1−Br2 99.06(2), N1−In1−Br1 86.385, N1−In1−Br2 92.49(10), N1−In1−N1 171.04(16).

Compound **3** exists as a molecular *mer*-$InBr_3Py_3$ (Figure 3) with coordination number 6 of indium, similar to known

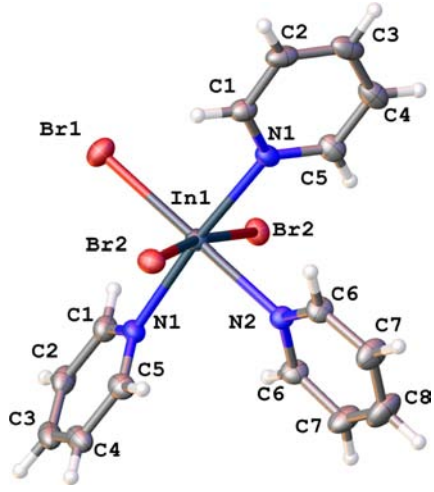

Figure 3. Molecular structure of complex $InBr_3Py_3$ (**3**) in the crystal. Selected interatomic distances (Å): In1−N1 2.293(2), In1−N2 2.313(3), In1−Br1 2.6050(4), In1−Br2 2.6436(3). Selected bond angles (deg): N1−In1−N1 174.50(7), N1−In1−N2 87.25(5), N1−In1−Br1 92.75(5), N1−In1−Br2 89.21(5), N2−In1−Br1 180.00(2), N2−In1−Br2 85.54(1), Br1−In1−Br2 94.46(1).

analogs $AlCl_3Py_3$,[8] $InCl_3Py_3{\cdot}Py$,[11] $InBr_3Py_3{\cdot}Py$,[12] InI_3Py_3,[13] $TlCl_3Py_3{\cdot}Py$, and [11] $TlBr_3Py_3$.[14] Note that the previously structurally characterized compound $InBr_3Py_3{\cdot}Py$[12] contained additional noncoordinated Py molecules in the crystal lattice. A synthesis in vacuum by condensation of pyridine to $InBr_3$ allowed to obtain **3** as a solvent-free sample. The molecular

dx.doi.org/10.1021/ic402162d | *Inorg. Chem.* 2013, 52, 13207−13215

Table 2. Comparison of Experimental (X-ray) Bond Distances in Solid 1−3 and Computed B3LYP/def2-TZVP Values for the Gas Phase Complexes

	r(In−N) (Å)			r(In−Br) (Å)		
compound	X-ray	B3LYP	$\Delta_{(comp-exp)}$	X-ray	B3LYP	$\Delta_{(comp-exp)}$
1	2.194(7)	2.310	0.116	2.4690(11)	2.504	0.035
				2.4697(10)	2.508	0.038
				2.4855(11)	2.509	0.023
2	2.275(5)	2.379	0.104	2.5857(6)	2.596	0.010
				2.7609(6)	2.842	0.081
3	2.293(2)	2.409	0.116	2.6050(4)	2.593	−0.012
	2.313(3)	2.527	0.214	2.6436(3)	2.654	0.010

parameters of the octahedral *mer*-$InBr_3Py_3$ unit, found in the present work, are in good agreement with previously reported ones for $InBr_3Py_3 \cdot Py$.[12]

The obtained results allow us to discuss trends in structural parameters in the $InBr_3Py_x$ series (x = 1−3). Both In−N and terminal In−Br distances increase with the increasing number of Py ligands, coordinated to indium (Table 2). The same trends are observed in the $AlCl_3Py_x$ series as well.[6,8]

The planar In_2Br_6 unit, found in **2**, is unprecedented among group 13 metal halide complexes with Py. The existence of a dimeric $In_2Br_6Py_4$ instead of the expected monomeric $InBr_3Py_2$ or ionic $[InBr_2Py_4]^+[InBr_4]^-$ is puzzling. Note that valence-isoelectronic analogs of group 17 and 15 elements also exist as dimers I_2Cl_6[32] and $As_2Cl_6 \cdot 2PMe_3$.[33] Thus, the structure of **2** fits to the structural pattern of dimeric planar fragments of group 17, 15, and 13 elements (Scheme 1). To address the question of the stability of dimeric $In_2Br_6Py_4$ and its analogs, theoretical studies have been carried out.

Scheme 1. Schematic Representation of the 12-Electron Valence Shell for Group 17, 15, and 13 Elements in Structures Featuring Dimeric E_2X_6 Fragment (L = Lewis Base)

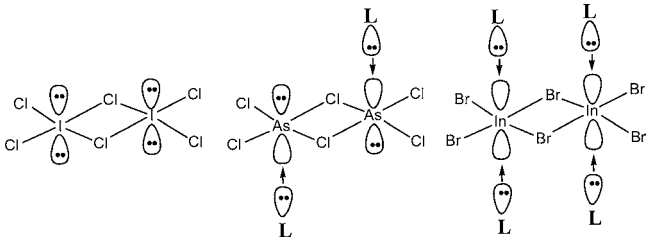

Quantum Chemical Studies. Optimized geometries for the considered gas phase complexes in the $InBr_3Py_x$ series (x = 1−3) are given in Figure 4. The meridional isomer of $InBr_3Py_3$ is predicted to be by 34 kJ mol^{-1} more stable than the facial one, in agreement with experimental findings for **3**. Optimized gas phase geometries are in satisfactory agreement with experimental data for the solid state complexes (Table 2). Computed In−N distances for gaseous complexes are over-estimated by 0.1−0.2 Å compared to experimental data in the solid state, which is expected due to shortening of the donor−acceptor bonds on going from gas phase to the condensed phase.[34] The difference between computed and experimental In−Br distances is much smaller (0.01−0.04 Å), only for **2** the maximal difference for the bridging In−Br bond length amounts to 0.08 Å (Table 2).

The energetic characteristics of the processes are summarized in Table 3. The computed gas phase enthalpies for subsequent Py elimination from $InBr_3Py_x$ are endothermic by 20, 13, and 96 kJ mol^{-1} for x = 3, 2, and 1, respectively. Because dissociation is entropically favorable, gaseous **3** and **2** should easily lose excess of pyridine upon heating, which agrees well with our tensimetry studies (vide infra). It should be noted that gaseous $In_2Br_6Py_4$ (Figure 4c) is metastable because its dissociation into monomeric $InBr_3Py_2$ (Figure 4b) is predicted to be exothermic by 50 kJ mol^{-1}, in stark contrast to the experimentally observed dimeric structure of **2** in the solid state.

We have also computed donor and acceptor reorganization energies upon complex formation and derived intrinsic values of the donor−acceptor (DA) bond energy (Table S5, Supporting Information). The average DA bond energy in the dimeric $In_2Br_6Py_4$ is 93 kJ mol^{-1}, larger than in the monomeric $InBr_3Py_2$ (80 kJ mol^{-1}). Thus, formation of the $In_2Br_6Py_4$ dimer is favored in terms of In−N bond energy. However, the reorganization energy of $InBr_3$ in monomeric $InBr_3Py_2$ is small (12 kJ mol^{-1}) compared to the large reorganization energy of In_2Br_6 in dimeric $In_2Br_6Py_4$ (187 kJ mol^{-1}). Apparently, high reorganization energy of In_2Br_6 into the planar form makes formation of $In_2Br_6Py_4$ in the gas phase energetically unfavorable. Thus, the existence of **2** in form of $In_2Br_6Py_4$ dimers can only be attributed to the solid state stabilization.

To elucidate the stability of $M_2X_6Py_4$ complexes for other group 13 analogs, the geometries of monomeric MX_3Py_2 and dimeric $M_2X_6Py_4$ species have been optimized (M = Al, Ga, In, Tl; X = Cl, Br). It should be noted that in case of the gallium and thallium derivatives, the $M_2X_6Py_4$ structure with planar M_2X_6 unit turned out to be either a transition state (GaX_3, $TlCl_3$) or the second-order stationary point ($TlBr_3$). Optimization without symmetry constrains leads to van der Waals bound MX_3Py_2 dimers. Thus, the Ga and Tl dimeric complexes are not minima on PES and should dissociate into monomers. This is in good agreement with experimentally observed structure of monomeric $TlBr_3Py_2$ in the solid state.[14] For aluminum and indium, the $M_2X_6Py_4$ structures are true minima on PES. Such a difference may be related to the secondary periodicity.[35]

Computational data reveal that all $M_2X_6Py_4$ dimers are metastable with respect to the dissociation into monomers (Table S4, Supporting Information). It is worthwhile to compare the energetics of the dissociation with data for their valence-isoelectronic analogs of group 17 and 15 elements. To this end, structures of group 17 and 15 compounds I_2Cl_6, $E_2Cl_6Py_2$ (E = As, Sb) and their respective monomers have been optimized. The experimentally known compound $As_2Cl_6(PMe_3)_2$[33] was also studied for comparison. The optimized structures of In_2Cl_6, $Sb_2Cl_6Py_2$, and $In_2Cl_6Py_4$ are

dx.doi.org/10.1021/ic402162d | Inorg. Chem. 2013, 52, 13207−13215

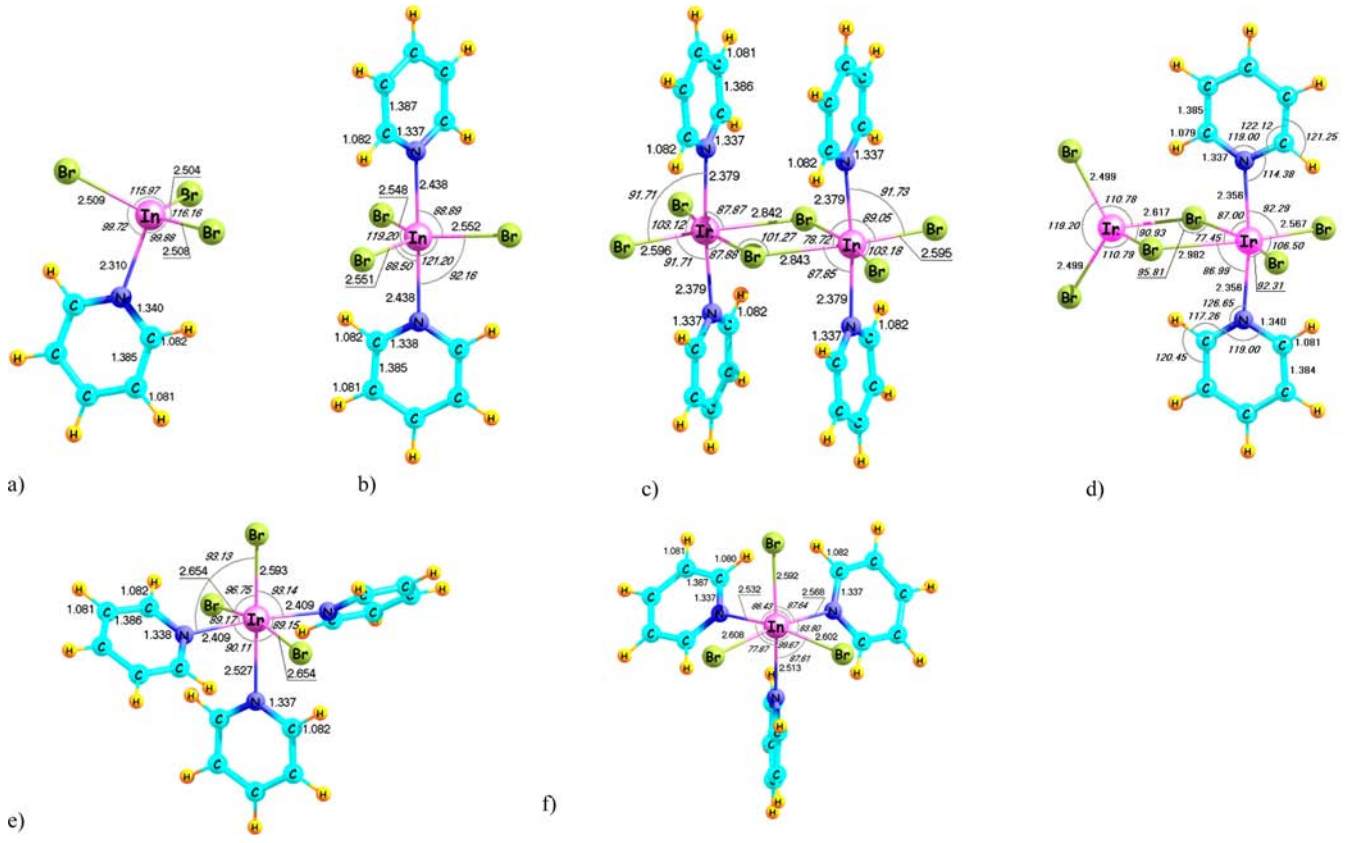

Figure 4. B3LYP/def2-TZVP optimized geometries of complexes: (a) $InBr_3Py$; (b) $InBr_3Py_2$; (c) $In_2Br_6Py_4$; (d) $In_2Br_6Py_2$; (e) *mer*-$InBr_3Py_3$; (f) *fac*-$InBr_3Py_3$.

Table 3. Computed Thermodynamic Properties for Dissociation of Gas Phase Complexes[a]

process	ΔH°_{298}	ΔS°_{298}	ΔG°_{298}
mer-$InBr_3Py_3$ = (1/2)$In_2Br_6Py_4$ + Py	19.8	65.3	0.3
(1/2)$In_2Br_6Py_4$ = $InBr_3Py_2$	−24.9	120.8	−58.0
$InBr_3Py_2$ = $InBr_3Py$ + Py	37.4	148.9	−7.0
(1/2)$In_2Br_6Py_4$ = $InBr_3Py$ + Py	12.5	1.3	12.1
$InBr_3$ Py = $InBr_3$ + Py	95.8	141.8	53.6
$In_2Br_6Py_4$ = $InBr_3Py$ + *mer*-$InBr_3Py_3$	−7.3	−64.0	11.8
$In_2Br_6Py_4$ = $In_2Br_6Py_2$ + 2Py	53.5	348.6	−50.4
$In_2Br_6Py_2$ = $2InBr_3Py$	−28.6	170.9	−79.5
$In_2Br_6Py_2$ = In_2Br_6 + 2Py	96.2	311.9	3.3

[a]Standard enthalpies (ΔH°_{298}) and Gibbs energies (ΔG°_{298}) in kJ mol^{-1}; standard entropies (ΔS°_{298}) in J mol^{-1} K^{-1}. B3LYP/def2-TZVP level of theory.

given in Figure 5. Planar D_{2h} symmetric I_2Cl_6 is a transition state with respect to puckering at B3LYP/def2-TZVP level of theory, in contrast to the solid state structure.[32] Optimization without symmetry constraints yields a minimum structure (Figure 5a). It exhibits two planar ICl_4 moietes joined by a common edge, with a dihedral angle between planes of 12°. This structure is only by 0.3 kJ mol^{-1} lower in energy than the perfectly planar transition state of D_{2h} point group. The nonplanar structure of I_2Cl_6 was also reported at B3LYP/3-21G* level of theory.[36] Due to ambiguous DFT results, we have redetermined the molecular structure of I_2Cl_6 (**4**) in the solid state. Our findings (Figure 6) reveal a perfectly planar molecule in agreement with the earlier study.[32] The sum of angles around iodine is 359.97 ± 0.04, indicating square planar geometry. For reason of the ambiguous DFT results, the data were also refined against a model in the *P*1 space group. In this space group, the molecule is also planar within the standard deviation of 0.3°. Geometry optimization at MP2/def2-TZVP level of theory revealed that D_{2h} symmetric structure of I_2Cl_6 is a true minimum on PES.

We have also optimized the structures of the bromine analogs I_2Br_6 and $Sb_2Br_6Py_2$. The experimentally unknown I_2Br_6 is predicted to be perfectly planar with a sizable endothermic dissociation enthalpy into IBr_3 monomers of 71 kJ mol^{-1}. The antimony analog $Sb_2Br_6Py_2$ is also stable with respect to dissociation into monomeric $SbBr_3Py$ (Table 4). Thus, these molecules should exist in dimeric forms at low temperatures. Interestingly, our computations predict that I_2Br_6 is also energetically stable with respect to the dissociation into IBr and Br_2 (dissociation enthalpy of 18 kJ mol^{-1} per mole of I_2Br_6), but taking the entropy factor into account, I_2Br_6 is predicted to be thermodynamically stable only below 50 K.

The central atom of all these compounds formally possesses a 12-electron valence shell (Scheme 1), which exceeds the Lewis octet rule. Thus, such compounds may be considered as hypervalent. However, as shown by Noury, Dilvi, and Gillespie,[37] in the experimentally known hypervalent compounds the actual population of the valence shell is smaller than eight due to electronegativity of substituents, which adopt an excess charge. We have performed an NBO analysis[38] of **2** and related group 17 and 15 dimers. According to NBO analyses, the valence shell occupation of the central atom decreases in order: I_2Cl_6 (5.87) > $Sb_2Cl_6Py_2$ (3.50) > $In_2Cl_6Py_4$ (1.54). The population of Cl atoms (7.3−7.6 electrons in valence shell) does not change much within the series. Analogous results were

dx.doi.org/10.1021/ic402162d | *Inorg. Chem.* 2013, 52, 13207−13215

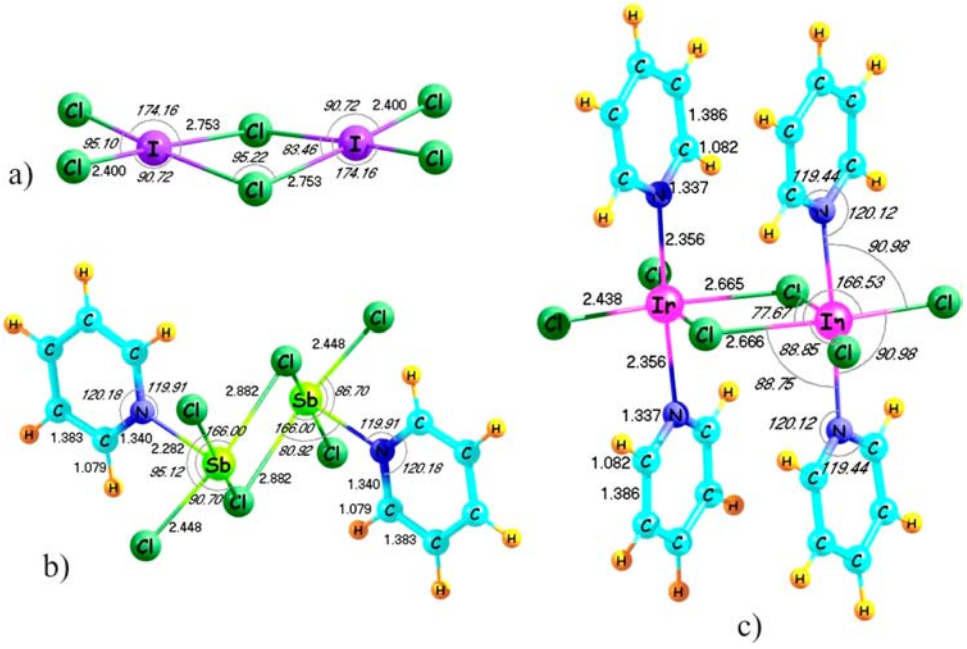

Figure 5. B3LYP/def2-TZVP optimized geometries of (a) I_2Cl_6, (b) $Sb_2Cl_6Py_2$, and (c) $In_2Cl_6Py_4$.

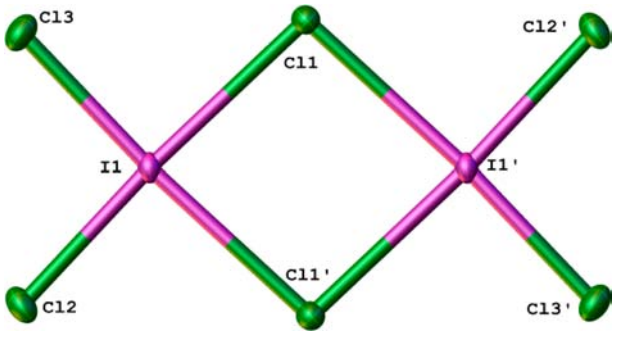

Figure 6. Molecular structure of I_2Cl_6 (**4**) in the crystal. Selected interatomic distances (Å): Cl1−I1 2.7103(5), I1−Cl2 2.3464(6), I1−Cl3 2.3646(6), I1−I1′ 4.0056(4), Cl1−Cl1′ 3.7256(10). Selected bond angles (deg): Cl3−I1−Cl2 93.27(2), Cl3−I1−Cl1 90.542(18), Cl2−I1−Cl1 90.311(19), Cl1−I1−Cl1′ 85.851(16), I1−Cl1−I1′ 94.149(16).

Table 4. Computed Gas Phase Thermodynamic Properties for Dissociation of Valence-Isoelectronic Group 13, 15, and 17 Dimeric Molecules into Monomers[a]

process	ΔE°_0	ΔH°_{298}	ΔS°_{298}	ΔG°_{298}
$I_2Cl_6 = 2ICl_3$	72.0	67.3	142.0	24.9
$Sb_2Cl_6Py_2 = 2SbCl_3Py$	58.4	53.2	175.6	0.9
$As_2Cl_6Py_2 = 2AsCl_3Py$	45.1	39.9	162.5	−8.5
$As_2Cl_6(PMe_3)_2 = 2AsCl_3PMe_3$	32.6	27.6	165.3	−21.6
$In_2Cl_6Py_4 = 2InCl_3Py_2$	−26.5	−30.9	210.8	−93.7
$I_2Br_6 = 2IBr_3$	75.7	70.7	163.1	22.0
$Sb_2Br_6Py_2 = 2SbBr_3Py$	55.5	49.8	182.2	−4.5
$In_2Br_6Py_4 = 2InBr_3Py_2$	−44.9	−49.8	221.6	−115.9

[a]Reaction energies (ΔE°_0), standard enthalpies (ΔH°_{298}), and Gibbs energies (ΔG°_{298}) in kJ mol^{-1}; standard entropies ΔS°_{298} in J mol^{-1} K^{-1}. B3LYP/def2-TZVP level of theory.

obtained for the bromine analogs I_2Br_6 (6.13), $Sb_2Cl_6Py_2$ (3.68), and $In_2Br_6Py_4$ (1.76). Thus, the central atoms in the studied compounds contain less than 8 electrons in their valence shell and should not be considered as hypervalent. Apparently, an increase of the electronegativity differences between central and terminal atoms in this row results in a depopulation of the valence shell of the least electronegative central atom.

Computational studies allow us to conclude that, in contrast to group 17 and 15 valence-isoelectronic analogs, the observed dimeric structure of **2** arises rather from the solid state stabilization.

Tensimetry Studies. To obtain thermodynamic parameters for vaporization and dissociation of **1**−**3**, a series of vapor pressure−temperature dependence measurements have been performed by the static tensimetry method with a glass membrane null-manometer.[2,22] Details on tensimetry apparatus are given in the Supporting Information. Six tensimetric experiments with molar ratios $InBr_3$:Py = 1:1.0, 1:1.1, 1:2.1, 1:2.9, 1:3.4, and 1:5.0 have been performed. They will be referred to as experiments 1−6, respectively. In all experiments, Py was introduced first and its exact amount was established on the basis of thermal expansion line in an unsaturated vapor region: $n = PV/(RT)$. After that, the compartment with $InBr_3$ was mechanically broken and the system was stored at room temperature for about 12−48 h. For each tensimetry experiment, several series of measurements of vapor pressure−temperature dependence have been performed (see Supporting Information for details). In experiments 1 and 2, noticeable vapor pressure appears only above 470 K (Figure S3, Supporting Information), which indicates that the solid $InBr_3Py$ complex has low volatility and does not dissociate below this temperature. Because $InBr_3$ has negligible vapor pressure at the studied temperature interval ($InBr_3$ sublimes without melting and has a vapor pressure of 0.1 Torr at 515 K, sublimation enthalpy is 147 ± 4 kJ mol^{-1} [39]), we may assume that Py is the only gaseous form existing in the system at temperatures below 470 K. Thus, the amount of gaseous Py can be derived from the measured vapor pressure at a given temperature, which allows to determine the amount of the complexed Py in the solid state. Because the amount of introduced $InBr_3$ is known, the complex

dx.doi.org/10.1021/ic402162d | Inorg. Chem. 2013, 52, 13207−13215

composition in the solid state (the parameter x in formulas $InBr_3Py_x$) can be unambigously determined at each temperature (Figure 7). In excess pyridine, the complex $InBr_3Py_3$ (**3**)

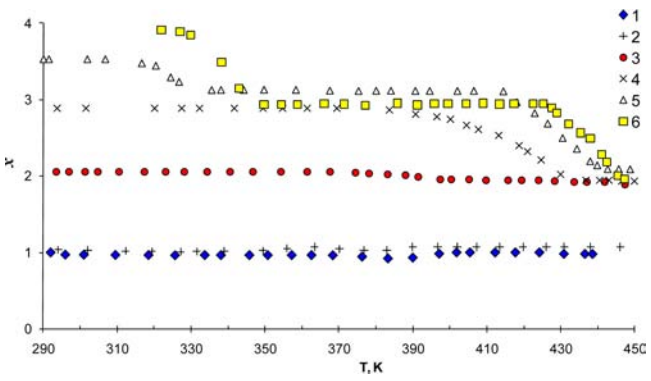

Figure 7. Solid state complex composition (parameter x in $InBr_3Py_x$) as function of temperature for experiments 1–6.

is stable with respect to Py loss up to 380 K. Heating to 610 K, an irreversible thermal destruction of pyridine (black coloring on the walls of the system) was observed. This indicates a catalytical role of indium tribromide in pyridine thermolysis, because pure pyridine decomposes at much higher temperatures (1200–1600 K[40]).

Tensimetric study allowed us to obtain the thermodynamic characteristics for several processes, listed in Table 5 (see Supporting Information for details). To characterize the vapor composition over $InBr_3Py_x$, mass spectrometry studies have been performed.

Mass Spectrometric Study. The vapor composition over samples with molar ratio $InBr_3$:Py 1:1.0, 1:2.1, and 1:2.9, identical to the tensimetry experiments 1, 3, and 4, respectively, were investigated by mass spectrometry. Measurements were carried out on a ThermoScientific ISQ mass spectrometer with a direct insert probe controller. An electron ionization energy of 70 eV was used. After synthesis in a vacuum system, samples were placed into thin glass capillaries. Those were opened immediately prior to the measurements. The mass spectra of the samples were continuously measured at 413 K (for 4 min), 433 K (for 4 min), and 453 K (for 4 min). For all studied compositions, the mass spectra over the liquid phase (453 K) are very similar (Table S1, Supporting Information), which suggests that the Py evolution takes place in the course of the MS experiment. The resulting samples are essentially enriched by $InBr_3$. The $InBr_2Py^+$ ion has the most intensive signal for all samples, which suggests that monomeric $InBr_3Py$ molecules are present in vapors at these conditions. The ion $InBr_2Py_2^+$ has the second highest intensity in the mass spectrum. Because the molecular mass of Py (79) coincides with the atomic mass of ^{79}Br, the distinction between ions has been made by analysis of isotope pattern (Figures S7–S9, Supporting Information). Ions containing more than two pyridine ligands were not observed. The observation of $InBr_2Py_2^+$ hints to a vaporization of species containing two Py ligands. Two possible pathways for the generation of $InBr_2Py_2^+$ ions are possible: a fragmentation of monomeric $InBr_3Py_2$ molecule and a fragmentation of dimeric $In_2Br_6Py_2$. The detection of $In_2Br_5Py_2^+$ ions (with low intensity) suggests that dimeric $In_2Br_6Py_2$ molecules are present in vapors. $InBr_2Py_2^+$, $In_2Br_4Py_2^+$, and $In_2Br_5Py^+$ might originate from further fragmentation of $In_2Br_5Py_2^+$. Note that traces of $In_2Br_5Py_2^+$ (1.4×10^{-4}%) and significant amounts of $InBr_2Py_2^+$ (52%) are detected in the mas spectra of the sample with a 1:1 composition (Table S1, Supporting Information). Supposedly, $InBr_3Py$ is partially ionized in the melt, which can give rise to metastable $In_2Br_6Py_2$ dimers:

$$[InBr_2Py_2]^+(l) + [InBr_4]^-(l) \leftrightarrows In_2Br_6Py_2(l) \leftrightarrows 2InBr_3Py(l)$$

Note that the bridging In–Br distances in the optimized structure of $In_2Br_6Py_2$ (Figure 4d) are quite unequal; the one with tetrahedral In (c.n. 4) is 0.36 Å shorter than the one with octahedral In (c.n. 6). The latter distance of 2.982 Å is significantly larger than the computed 2.834 Å for $In_2Br_6Py_4$ and 2.694 Å for dimeric In_2Br_6. Such long distances are indicative of In–Br bond weakening, which will facilitate ionization of dimeric molecule in the melt with formation of $[InBr_2Py_2]^+$ and $[InBr_4]^-$.

The existence of the dimeric molecule $In_2Br_6Py_2$ in the gas phase is intriguing, because complexes of aluminum and gallium halides with pyridine vaporize in the monomeric form and exist in vapors as individual MX_3Py molecules, which dissociate upon heating.[41] Computational studies reveal that, among the possible isomers of $In_2Br_6Py_2$, only the isomer with Py ligands attached to the same In atom turned out to be minimum on PES (Figure 4d). Optimization attempts for the alternative symmetric isomer (Py ligands coordinated to different In atoms) resulted in two $InBr_3Py$ monomers, weakly bound by van der Waals interactions in a head-to-tail fashion. Thus, the symmetric 10 e^- valence shell dimer $In_2Br_6Py_2$ is not a minimum on PES, whereas the asymmetric 8 and 12 e^- valence shell isomer (Figure 4d) is a true minimum on PES. Interestingly, similar situation is also observed for valence-isoelectronic group 15 dimers E_2X_6 (E = As, Sb; X = Cl, Br). The E_2X_6 dimers with a 10 e^- valence shell are not minima on PES and dissociate into EX_3 monomers upon geometry optimization, whereas group 15 donor-stabilized 12 e^- valence shell dimers $E_2X_6L_2$ (L = Py, PMe_3) are local minima on respective PES. The optimized structure of $As_2Cl_6(PMe_3)_2$ (Figure S11g, Supporting Information) is in good agreement with the experimental data.[33] Note that the 8 e^- valence shell dimers of group 13 analogs E_2X_6 (E = Al, Ga; X = Cl, Br) are stable gas phase species.[42] Our results indicate that dimerization depends on the formal occupation of the valence shell: it is favored in the case of the 12 and 8 e^- valence shells but disfavored in the case of the 10 e^- valence shell.

CONCLUSIONS

The experimentally characterized structures of **1**–**3** represent the second example of the structurally characterized series of

Table 5. Thermodynamic Characteristics of the Processes Obtained by Tensimetry Method

process	temperature range (K)	T_{mean} (K)	ΔH°_T (kJ mol^{-1})	ΔS°_T (J mol^{-1} K^{-1})
$InBr_3Py_3{\cdot}Py(s) = InBr_3Py_3(s) + Py(g)$	325–345	330	34.7 ± 0.9	84.6 ± 2.7
$InBr_3Py_3(s) = (1/2)In_2Br_6Py_4(s) + Py(g)$	380–440	415	86.7 ± 2.3	189.4 ± 5.5
$In_2Br_6Py_4(l) = In_2Br_6Py_2(g) + 2Py(g)$	476–526	501	100 ± 11	126 ± 23

dx.doi.org/10.1021/ic402162d | Inorg. Chem. 2013, 52, 13207–13215

MX_3Py_x adducts (x = 1−3) besides $AlCl_3Py_x$. In contrast to ionic $[AlCl_2Py_4]^+[AlCl_4]^-$ [8] and monomeric trigonal bipyramidal $TlBr_3Py_2$,[7] **2** exists as molecular dimer $In_2Br_6Py_4$ that features a planar In_2Br_6 unit and 12-electron valence shell for the indium atoms. This is only the second example of this structural type for group 13 metal halides besides Tl_2Cl_6(*N*-nicotinamide)$_4$. Such structures complete the series of dimeric valence-isoelectronic molecules of group 17, 15, and 13 elements featuring a planar E_2X_6 unit. Quantum chemical computations reveal that in contrast to the group 15 and 17 analogs, the molecular dimer $In_2Br_6Py_4$ is metastable with respect to dissociation into monomers.

Tensimetry studies of the $InBr_3$−Py system allowed us to determine the solid state complex composition at any given temperature. Complexes with high Py content easily lose Py upon heating, and thermodynamic characteristics for the processes of Py loss have been determined. Unlike other group 13 metal halide pyridine complexes, which are monomeric in vapors,[41] the mass spectrometric studies indicate the existence of dimeric $In_2Br_6Py_2$ molecules in vapor phase. Quantum chemical data evidence that such $In_2Br_6Py_2$ complex is metastable with respect to dissociation into $InBr_3Py$ monomers.

Halogen-bridged dimers of group 17, 15, and 13 elements with a formally 12 and 8 e^- valence shell of the central atom are stable or metastable, whereas 10 e^- valence shell halogen-bridged dimers are not minima on PES. This observation suggests that the formation of the 12 or 8 e^- valence shell is an important factor in formation of the dimeric complexes of heavier main group elements. Yet, unknown valence-isoelectronic dimeric I_2Br_6 and $Sb_2Br_6Py_2$ compounds are predicted to be stable with respect to the dissociation into monomers and can be regarded as possible synthetic targets.

■ ASSOCIATED CONTENT

Supporting Information

Summary of the performed tensimetry experiments, experimental data on vapor-pressure measurements, total energies, standard entropies and enthalpies, optimized structures and xyz coordinates for all studied compounds obtained at B3LYP/def2-TZVP level of theory (52 pages), and crystallographic information in CIF format. This information is available free of charge via Internet at http://pubs.acs.org.

■ AUTHOR INFORMATION

Corresponding Author

*A. Y. Timoshkin. E-mail: alextim@AT11692.spb.edu.

Notes

The authors declare no competing financial interest.

■ ACKNOWLEDGMENTS

I.V.K. is grateful to DAAD and SPbSU for joint fellowship "Dmitrii Mendeleev". A.Y.T. is grateful to Alexander von Humboldt foundation for reinvitation fellowship. Excellent services of Resource Center "Computer Center of SPbSU", Research Centers for Thermogravimetric and Calorimetric Research and Research Centers for X-ray Diffraction Studies of SPbSU are acknowledged. This work was financially supported by SPbSU grant 12.37.139.2011.

■ REFERENCES

(1) Gur'yanova, E. N.; Gol'dshtein, I. P.; Romm, I. P. *Donor-Acceptor Bond*; Halsted: New York, 1975.

(2) Davydova, E. I.; Sevastianova, T. N.; Suvorov, A. V.; Timoshkin, A. Y. *Coord. Chem. Rev.* **2010**, *254*, 2031.

(3) (a) Jones, A. C.; O'Brien, P. CVD of Compound Semiconductors. *Precursor Synthesis, Development and Applications*; VCH: Weinheim, Germany, 1997. (b) Malik, M. A.; Afzaal, M.; O'Brien, P. *Chem. Rev.* **2010**, *110*, 4417.

(4) Sevast'yanova, T. N.; Suvorov, A. V. *Russ. J. Coord. Chem.* **1999**, *25*, 679.

(5) Timoshkin, A. Y.; Bodensteiner, M.; Sevast'yanova, T. N.; Lisovenko, A. S.; Davydova, E. I.; Scheer, M.; Butlak, A. V. *Inorg. Chem.* **2012**, *51*, 11602.

(6) Dimitrov, A.; Heidemann, D.; Kemnitz, E. *Inorg. Chem.* **2006**, *45*, 10807.

(7) Jeffs, S. E.; Small, R. W. H.; Worrall, I. J. *Acta Crystallogr., Sect. C: Cryst. Struct. Commun.* **1984**, *40*, 65.

(8) Pullmann, P.; Hensen, K.; Bats, J. W. *Z. Naturforsch., B: Anorg. Chem., Org. Chem.* **1982**, *37*, 1312.

(9) Sinclair, I.; Small, R. W. H.; Worrall, I. J. *Acta Crystallogr., Sect. B: Struct. Crystallogr. Cryst. Chem.* **1981**, *37*, 1290.

(10) Toma, M.; Sanchez, A.; Castellano, E.; Berdan, I.; Garcia-Tasende, M. S. *Rev. Chim. (Bucharest, Rom.)* **2003**, *54*, 476.

(11) Jeffs, S. E.; Small, R. W. H.; Worrall, I. J. *Acta Crystallogr., Sect. C: Cryst. Struct. Commun.* **1984**, *40*, 1329.

(12) Small, R. W. H.; Worrall, I. J. *Acta Crystallogr., Sect. B: Struct. Crystallogr. Cryst. Chem.* **1982**, *38*, 932.

(13) Pardoe, J. A. J.; Cowley, A. R.; Downs, A. J.; Greene, T. M. *Acta Crystallogr., Sect. C: Cryst. Struct. Commun.* **2005**, *61*, m200.

(14) Jeffs, S. E.; Small, R. W. H.; Worrall, I. J. *Acta Crystallogr., Sect. C: Cryst. Struct. Commun.* **1984**, *40*, 1827.

(15) Downs, A. J., Ed. *The Chemistry of Aluminium, Gallium, Indium and Thallium*; Blackie: London, 1993.

(16) George, K.; Jura, M.; Levason, W.; Light, M. E.; Ollivere, L. P.; Reid, G. *Inorg. Chem.* **2012**, *51*, 2231.

(17) Habeeb, J. J.; Said, F. F.; Tuck, D. G. *J. Chem. Soc., Dalton Trans.* **1980**, 1161.

(18) Agilent Technologies. *CrysAlisPro software system*, different versions 2006−2012; Agilent Technologies UK, Ltd.: Oxford, U.K.

(19) Clark, R. C.; Reid, J. S. *Acta Crystallogr., Sect. A: Found. Crystallogr.* **1995**, *A51*, 887.

(20) Altomare, A.; Burla, M. C.; Camalli, M.; Cascarano, G. L.; Giacovazzo, C.; Guagliardi, A.; Moliterni, A. G. G.; Polidori, G.; Spagna, R. *J. Appl. Crystallogr.* **1999**, *32*, 115.

(21) Sheldrick, G. M. *Acta Crystallogr., Sect. A: Found. Crystallogr.* **2008**, *A64*, 112.

(22) Suvorov, A. V. *Termodinamicheskaya khimiya paroobraznogo sostoyaniya (Thermodynamic Chemistry of Vaporous State)*; Leningrad: Khimiiya, 1970 (in russian).

(23) Becke, A. D. *J. Chem. Phys.* **1993**, *98*, 5648.

(24) Lee, C.; Yang, W.; Parr, R. G. *Phys. Rev. B* **1988**, *37*, 785.

(25) Weigend, F.; Ahlrichs, R. *Phys. Chem. Chem. Phys.* **2005**, *7*, 3297.

(26) Timoshkin, A. Y.; Suvorov, A. V.; Bettinger, H. F.; Schaefer, H. F. *J. Am. Chem. Soc.* **1999**, *121*, 5687.

(27) Frisch, M. J.; Trucks, G. W.; Schlegel, H. B.; Scuseria, G. E.; Robb, M. A.; Cheeseman, J. R.; Scalmani, G.; Barone, V.; Mennucci, B.; Petersson, G. A.; Nakatsuji, H.; Caricato, M.; Li, X.; Hratchian, H. P.; Izmaylov, A. F.; Bloino, J.; Zheng, G.; Sonnenberg, J. L.; Hada, M.; Ehara, M.; Toyota, K.; Fukuda, R.; Hasegawa, J.; Ishida, M.; Nakajima, T.; Honda, Y.; Kitao, O.; Nakai, H.; Vreven, T.; Montgomery, J. A., Jr.; Peralta, J. E.; Ogliaro, F.; Bearpark, M.; Heyd, J. J.; Brothers, E.; Kudin, K. N.; Staroverov, V. N.; Kobayashi, R.; Normand, J.; Raghavachari, K.; Rendell, A.; Burant, J. C.; Iyengar, S. S.; Tomasi, J.; Cossi, M.; Rega, N.; Millam, J. M.; Klene, M.; Knox, J. E.; Cross, J. B.; Bakken, V.; Adamo, C.; Jaramillo, J.; Gomperts, R.; Stratmann, R. E.; Yazyev, O.; Austin, A. J.; Cammi, R.; Pomelli, C.; Ochterski, J. W.; Martin, R. L.; Morokuma, K.; Zakrzewski, V. G.; Voth, G. A.; Salvador, P.; Dannenberg, J. J.; Dapprich, S.; Daniels, A. D.; Farkas, Ö.;

Foresman, J. B.; Ortiz, J. V.; Cioslowski, J.; Fox, D. J. *Gaussian 09*, Revision A.1; Gaussian, Inc.: Wallingford, CT, 2009.
(28) Cheng, Q. M.; Stark, O.; Merz, K.; Winter, M.; Fischer, R. A. *J. Chem. Soc., Dalton Trans.* **2002**, 2933.
(29) Kühner, S.; Hausen, H.-D.; Weidlein, J. *Z. Anorg. Allg. Chem.* **1998**, *624*, 13.
(30) Staffel, T.; Meyer, G. *Z. Anorg. Allg. Chem.* **1988**, *563*, 27−37.
(31) (a) Berg, R. W.; Poulsen, F. W.; Nielsen, K. *Acta Chem. Scand.* **1997**, *51*, 442. (b) Troyanov, S. I.; Krahl, T.; Kemnitz, E. *Z. Kristallogr.* **2004**, *219*, 88.
(32) Boswljk, K. H.; Wiebenga, E. H. *Acta Crystallogr.* **1954**, *7*, 417.
(33) Hill, N. J.; Lewason, W.; Reid, G. *J. Chem. Soc., Dalton Trans.* **2002**, 1188.
(34) Leopold, K. R.; Canagaratna, M.; Phillips, J. A. *Acc. Chem. Res.* **1997**, *30*, 57.
(35) (a) Biron, E. V. *Zh. Russ. Fiz.-Khim. O-va.* **1915**, *47*, 964. (b) Frąckiewicz, K.; Czerwiński, M.; Siekierski, S. *Eur. J. Inorg. Chem.* **2005**, 3850.
(36) Poleshchuk, O. Kh.; Kalinina, E. L.; Latosińska, J. L.; Koput, J. *J. Mol. Struct. (Theochem)* **2001**, *574*, 233−243.
(37) Noury, S.; Dilvi, B.; Gillespie, R. J. *Inorg. Chem.* **2002**, *41*, 2164.
(38) Glendening, E. D.; Reed, A. E.; Carpenter, J. E.; Weinhold, F. *Gaussian NBO*, Version 3.1; Gaussian, Inc.: Wallingford, CT.
(39) Brunetti, B.; Palchetti, C.; Piacente, V. *J. Mater. Sci. Lett.* **1997**, *16*, 1395.
(40) Kiefer, J. H.; Zhang, O.; Kern, R. D.; Yao, J.; Jursic, B. *J. Phys. Chem. A* **1997**, *101*, 7061.
(41) (a) Timoshkin, A. Y.; Grigoriev, A. A.; Suvorov, A. V. *Russ. J. Gen. Chem.* **1995**, *65*, 1634. (b) Timoshkin, A. Y.; Suvorov, A. V.; Misharev, A. D. *Russ. J. Gen. Chem.* **2002**, *72*, 1874.
(42) Hargittai, M. *Chem. Rev.* **2000**, *100*, 2233.